Transactions, SMiRT-26
Berlin/Potsdam, Germany, July 10-15, 2022
Division VII

DEVELOPMENT AND APPLICATION OF EARTHQUAKE-TYPE DEPENDENT FRAGILITY CURVE

Sei'ichiro Fukushima[1], Akira Satoda[2], Masami Oshima[3]

[1] CEO, RKK Consulting, Tokyo Japan (fukushima@rkk-c.co.jp)
[2] Senior Engineer, Chiyoda Corporation, Kanagawa, Japan
[3] Senior Consultant, Chiyoda Corporation, Kanagawa, Japan

ABSTRACT

So far, authors have conducted probabilistic risk analysis of plant structures using seismic fragility curve whose ground motion index is the peak ground acceleration (hereinafter referred as PGA). Since the spectral characteristics of ground motion are earthquake specific, employing only PGA as an index may bring the large uncertainty in damage evaluation. The multi-event approach in which independent ground motions of numerous earthquakes are generated is one of approaches to reduce the uncertainty. However, the approch is time consuming and improper to obtain damage probability with high accuracy. On the basis that earthquake type controls the ground motion characteristics, this paper proposes earthquake-type dependent fragility curves that are combined earthquake-type dependent seismic hazard to reduce the uncertainty.

This paper establishes the earthquake-type dependent fragility curve by analytical way. Namely, the fragility curve is established using a set of ground motions whose spectral characteristics are accordance with the given earthquake type, such as crustal, inter-plate or intra plate earthquake.

Yokkaichi Industrial Complex in Mie prefecture is selected as model plant site, since the Yokkaichi city in Mie prefecture is in the vicinity of various types of earthquakes such as many active faults and the Nankai Trough. And, two towers that have different natural period are selected as model structures.

Comparison of fragility curve regarding to earthquake type showed that fragility curves are deferent if the earthquake-type of concern is different. So, it can be concluded that it is rational and adequate to use fragility curves corresponding to earthquake type. This conclusion was also proved by comparing risk curves.

INTRODUCTION

So far, authors have conducted probabilistic risk analysis of plant structures using seismic fragility curve whose ground motion index is the peak ground acceleration (PGA). Since the spectral characteristics of ground motion are earthquake specific, employing only PGA as an index may bring the large uncertainty in damage evaluation.

The multi-event approach in which independent ground motions of numerous earthquakes are generated is one of approaches to reduce the uncertainty. However, the approch is time consuming and improper to obtain damage probability with high accuracy, since it requires Monte-Carlo simulations.

On the basis that earthquake type controls the ground motion characteristics, this paper proposes earthquake-type dependent fragility curves that are combined earthquake-type dependent seismic hazard to reduce the uncertainty.

CONCEPT OF ESTABLISHING SEISMIC FRAGILITY CURVE

In the development of seismic fragility curve, two kinds of approaches are generally employed; the one is empirical and the other is analysis-based. The empirical approach has been widely used since 1995 Kobe earthquake. The advantage of the method is that it can include various effects which are difficult to consider and to model. On the other hand, the disadvantage is that the results are data dependent so that the result may not be adequate in different situation. The advantage and disadvantage of the analysis-based approach are reverse of ones by empirical approach.

This paper employs the analysis-based approach since there is few data of past damages to structures in order to examine the relationship between earthquake types and damages to various type of structures.

SEISMIC HAZARD ANALYSIS FOR MODEL SITE

In order to conduct analysis-based fragility analysis, seismic hazard analysis for model site is conducted, followed by uniform hazard spectra (UHSs) corresponding to crustal, inter-plate and intra plate earthquakes. The obtained UHSs are used as target spectra for generating ground motions to obtain probabilistic response of structures by Monte-Carlo simulation (MCS).

Conditions of Analysis

Yokkaichi Industrial Complex in Mie prefecture is selected as model plant site as shown by National Research Institute for Earth Science and Disaster Resilience: NIED (2019) in Fig. 1, since the Yokkaichi city in Mie prefecture is located in the vicinity of many active faults and the Nankai Trough. It is noted that mega earthquakes have occurred on a 100-to-150-year recurrence period in the area along the Nankai Trough.

Seismic source model is constructed based on the database prepared by NIED to assure the accountability. And ground motion prediction equation in NIED (2009) is employed.

Figure 1. Location of the model site

Results of Seismic Hazard Analysis

Figure 2 shows the uniform hazard spectra by all earthquakes, crustal earthquakes, inter-plate earthquakes and intra-plate earthquakes, respectively. Legend in each figure shows the return period. From the figure it is seen that the uniform hazard spectrum by intra-plate earthquake is dominant when return period is short and the one by inter-plate earthquake is dominant when return period is long.

The shapes of UHSs are almost identical regarding to return period except for one of 10 years, so the shape of UHSs corresponding to return period of 1000 years are referred as target spectra for generation of input ground motion.

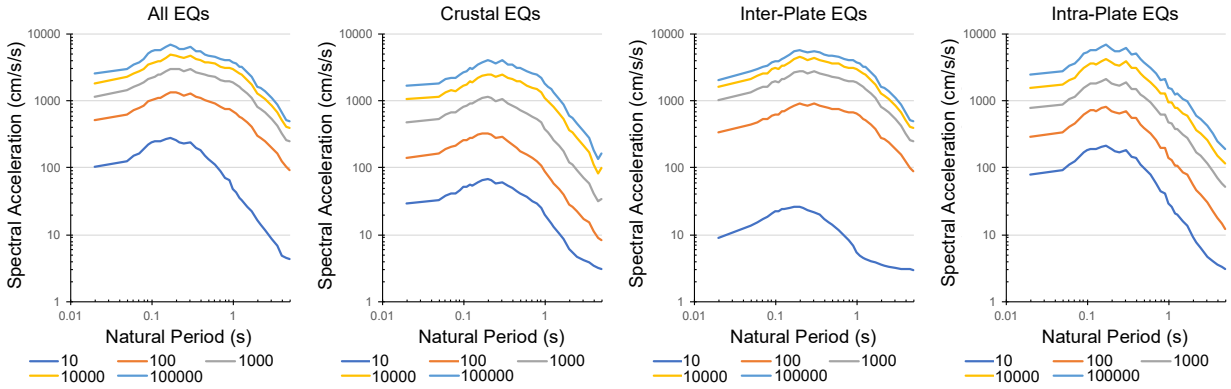

Figure 2. Uniform hazard spectra at Yokkaichi site

Figure 3 shows the Seismic hazard curves at the site. It is seen that the crustal and intra-plate earthquakes are dominant in the range that PGA is small. On the Contrary, inter-plate earthquake is dominant in case that PGA exceeds 200(cm/s/s).

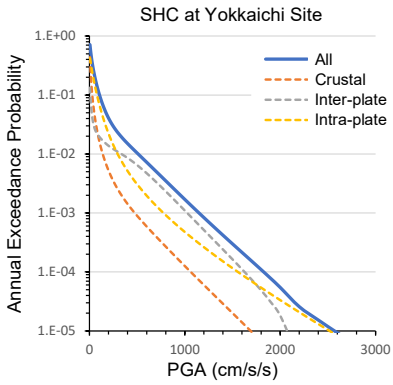

Figure 3. Seismic hazard curve at Yokkaichi site

Generation of Input Ground Motion for Seismic Fragility Analysis

Referring the spectral shape of UHSs corresponding to annual exceedance probability of 0.001, 200 response spectra are generated assuming that the standard deviation about the median UHS is 0.2 in common logarithm. Also assumed is the inter-period correlation by Tanaka et al. (2008), in which the correlation is given by Eq. (1),

$$\rho(t_1, t_2) = 1 - 0.308 \cdot abs\left[\ln\left(\frac{t_1}{t_2}\right)\right] \quad for\ t_1, t_2 \geq 0.1 \tag{1}$$

where, t_1 and t_2 are the periods of concern. In case t is smaller than 0.1, the correlation is assumed unity.

Figure 4 shows the 200 samples of response spectra of generated ground motions. It is noted that the median of peak ground acceleration is normalized by 100 (cm/s/s).

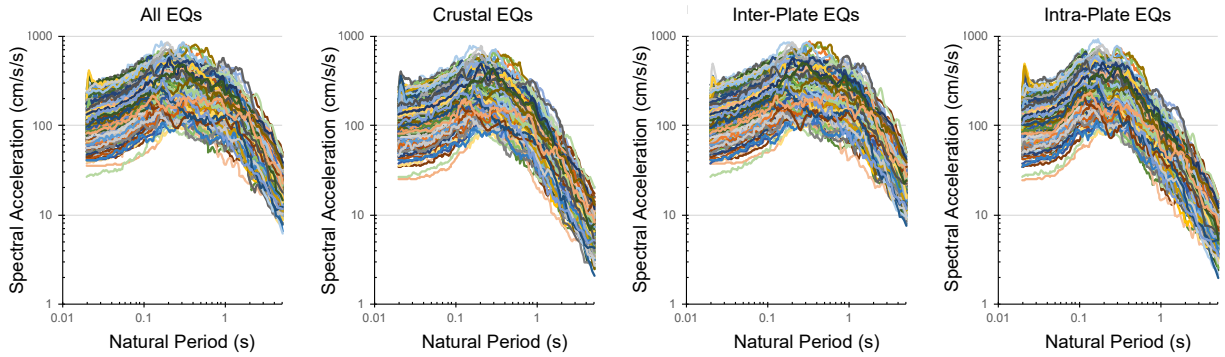

Figure 4. Response spectra of input ground motions for seismic fragility analysis

SEISMIC FRAGILUTY ANALYSIS OF MODEL STRUCTURES

Model Structures

Two towers supported on skirt are employed as modes structures whose specifications are summarized in Table 1. Towers are modelled as lumped mass model with fixed base, in which nodes are connected by linear beam elements. Specifications of models, such as mass, inertia, shear area and moment inertia are calculated using the data given in Table 1. Also given are Elastic modulus of material of 200,800 (N/mm2), Poisson's ratio of 0.3.

Table 1: Specification of towers

Item	Unit	Tower-1	Tower-2
High (Above the ground)	(mm)	10,000	30,000
Mean Diameter	(mm)	2,000	3,500
Thickness	(mm)	9	17
Operational Weight	(N/mm)	137.5	125.8

Result of Monta-Carlo Simulation

The results of MCS are summarized in Fig. 5, in which median and natural logarithm standard deviation of bending moment are shown. It is noted that the flexure is considered dominant as mentioned in Satoda et al. (2017), and the ground motion intensity used in the analysis is set to 100 (cm/s/s) for PGA.

Inter-plate earthquake and intra-plate earthquake are dominant for Tower-1 from the viewpoint of median, though the deference in response is not large. On the contrary, only inter plate-earthquake is dominant for Tower-2, since Tower-2 has longer natural period comparing to Tower-1 so that inter-plate earthquake excites the vibration of Tower-2. There is small deference in standard deviations, among which that by inter-plate earthquake is the smallest.

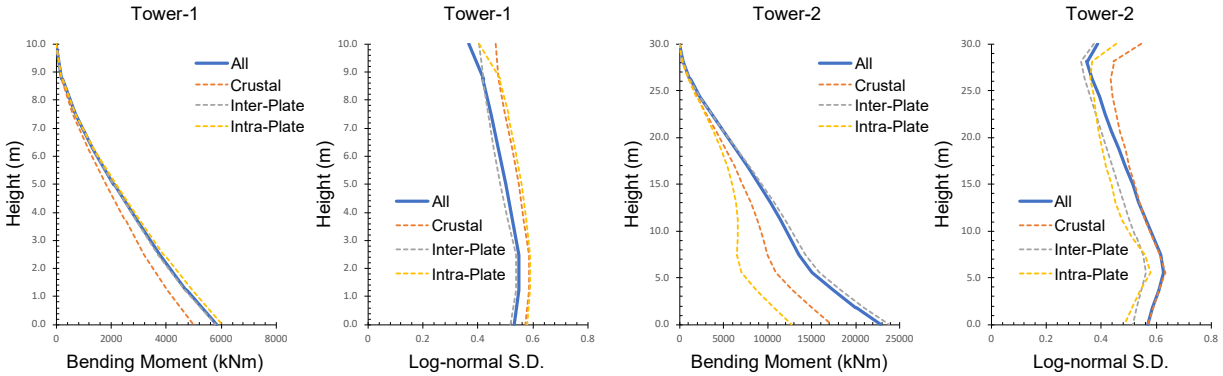

Figure 5. Response spectra of input ground motions for seismic fragility analysis

Evaluation of Seismic Fragility Curves

Seismic fragility of towers is assumed log-normally distributed, so that two parameters, median and log-normal standard deviation, are necessary to obtain seismic fragility curves (SFCs). SFC: $F(x)$ is given by Eq. (2),

$$F(x) = \Phi\left[\frac{\ln(x) - \ln(\bar{x})}{\zeta}\right] \tag{2}$$

where, $\Phi[\cdot]$ is normal distribution function, x is a ground motion intensity, $\bar{x}$ is a median capacity intensity, ζ is logarithmic standard deviation. It is noted that ζ is given in natural logarithm.

Authors assume that the failure of towers is dominated by flexural buckling, the median capacity intensity $\bar{x}$ is given by Eq. (3),

$$\bar{x} = \frac{\bar{M}}{m(x_R)} x_R = \frac{(\sigma_c - \sigma_0)Z}{m(x_R)} x_R \tag{3}$$

where, $\bar{M}$ is the median of buckling moment that is given by allowable buckling stress σ_c, permanent stress σ_c and section modulus Z. $m(x_R)$ is the median of resulting flexural moment for the input ground motion intensity x_R. Evaluation of σ_0 is based on the KHK (2012). Table 2 summarizes the parameters employed in Eq. (3).

Table 2: Summary of parameters used in Eq. (3)

Item	Unit	Tower-1	Tower-2
Allowable buckling stress σ_c	(N/mm^2)	165.00	165.00
Permanent stress σ_0	(N/mm2)	25.11	21.80
Section modulus Z	(m^3)	0.028	0.162
Median of buckling moment $\bar{M}$	(kN m)	3,920	23,197

Using the Eq. (3), the median capacity intensity $\bar{x}$ is calculated for each ground motion intensity. The natural log-normal deviation is given by response analysis as shown in Fig. 6. Other variability factors for capacity intensity, such as the variabilities in material strength and damping, are ignored, since they are negligible. Table 3 summarizes the acceleration capacity.

Table 3: Summary of acceleration capacity

Parameters in Eq. (3)	Unit	All		Crustal		Inter-Plate		Intra-Plate	
		T-1	T-2	T-1	T-2	T-1	T-2	T-1	T-2
x_R	(cm/s/s)	100	100	100	100	100	100	100	100
$m(x_R)$	(kN m)	4,729	17,427	4,026	12,876	4,679	18,340	4932	8721
$\bar{x}$	(cm/s/s)	82.9	133.1	97.4	180.2	83.8	126.5	79.5	266.0
ζ	-	0.548	0.610	0.587	0.610	0.538	0.547	0.588	0.543

Figure 6 compares the SFCs by earthquake type. SFC of Tower-1 will be overestimated for crustal earthquake and that of Tower-2 will also be overestimated for crustal and intra-plate earthquakes comparing to using fragility curve derived from all earthquakes. On the contrary, failure probability of Tower-2 will be somewhat underestimated for inter-plate earthquake.

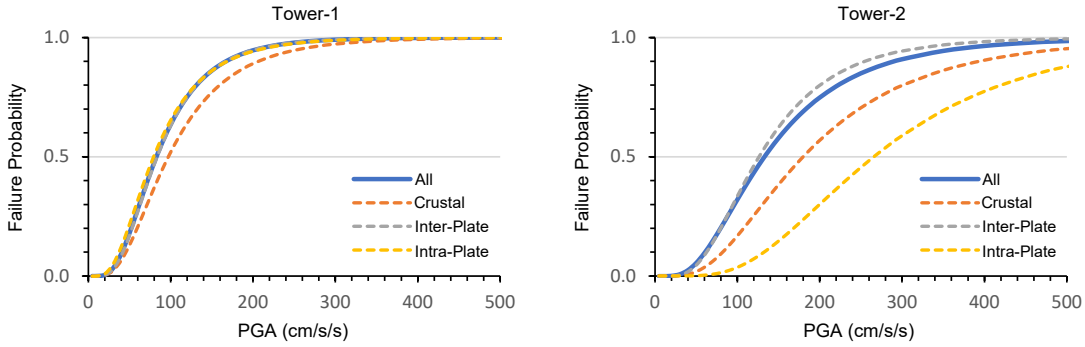

Figure 6. Comparison of fragility curves by earthquake-type

APPLICATION TO PROBABILISTIC RISK ANALYSIS

Comparison of Risk Analysis Method

The probabilistic seismic risk is often expressed by the risk curve (RC), which shoes the relationship between the risk parameter and its annual exceedance probability. In this paper the failure probability is used as a risk parameter. The simplest way to obtain the RC is to combine SHC and SFC by risk parameter. Figure 7shows some RCs. RC named "All" is obtained by combining SHC of "All" in Fig.3 and SFC of "All" in Fig.6. RCs named "Crustal", "Inter-PL" and "Intra-PL" are also obtained by the same way. It is noted that the RC named "All" is the one obtained previous method. RC named "Previous Method" is the one obtained by by Eq. (4),

$$p(y) = 1 - \sum_{i=1}^{3} (1 - p_i(y)) \tag{4}$$

where, y is the failure probability and $p(y)$ is its annual exceedance probability. $p_1(y)$, $p_2(y)$ and $p_3(y)$ are the annual exceedance probabilities corresponding to crustal, inter-plate and intra-plate earthquakes, respectively.

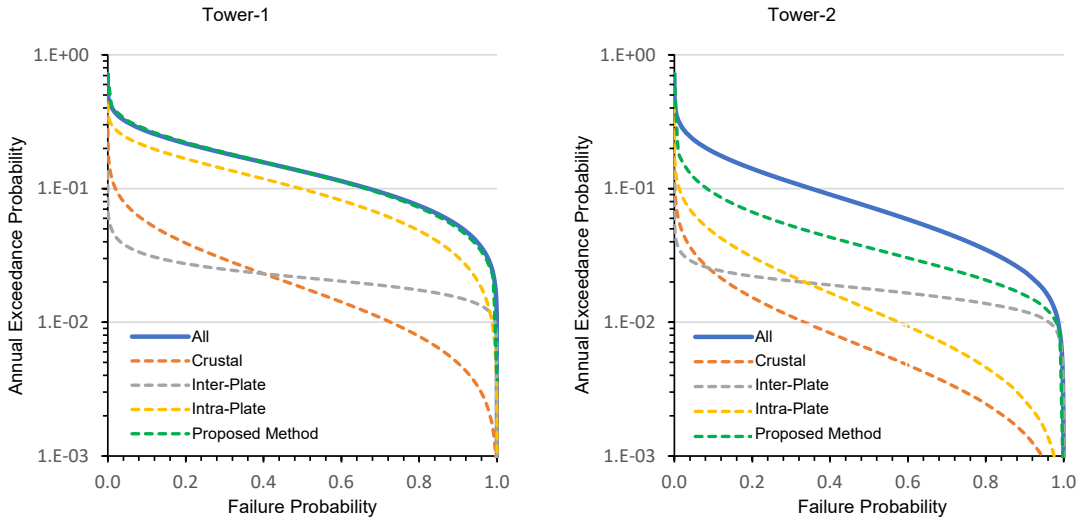

Figure 7. Comparison of risk curves

From the comparison, it is seen that the proposed method and the previous method give almost same RCs for Tower-1 since SFCs especially SFC for dominant inter-plate earthquake are identical with SFC for all earthquakes. On the contrary in case of Tower-2, the proposes method gives lower RC than the previous method does. This is because that the SFC for dominant inter-plate earthquake is much lower than the SFC for all earthquakes.

Adequacy of Proposed Risk Analysis Method

In order to examine the adequacy of proposed method, RCs obtained by previous and proposed method are compared with the one by multi-event model, whose flowchart is shown by Fig. 8. Multi-event model has been used to examine the RC of portfolio of buildings as Fukushima (2015). One of the features of the multi-event model is that it does not separate the risk analysis into hazard analysis part and fragility analysis part.

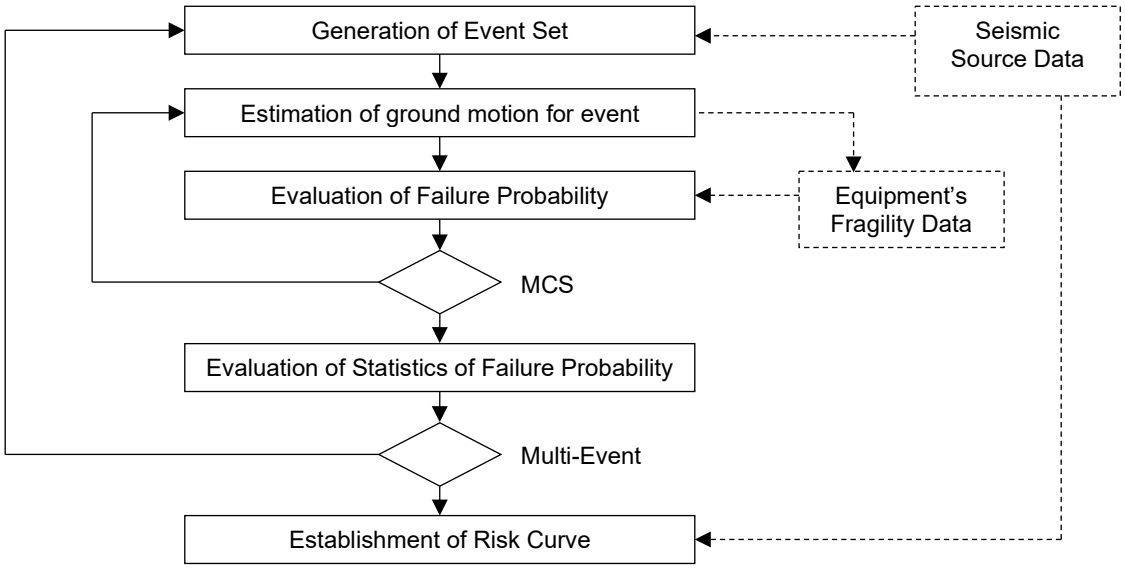

Figure 8. Flowchart of risk analysis using multi-event model

Let y_i be the risk value for event i. So annual exceedance probability of the risk value $p_j(y_i)$ for j^{th} threshold by event i is given by the following equation,

$$p_j(y_i) = \nu_i \cdot P(y_i > z_j) \tag{5}$$

where, ν_i is annual occurrence frequency of event i, z_j is j^{th} threshold. Since events are independent to one another, annual exceedance probability of the risk value $p(y)$ is given as follows,

$$p_j(y) = \sum_{i=1}^{n} p_j(y_i) \tag{6}$$

where, n is the number of events. RC can be obtained as the relationship between z_j and $p_j(y)$.

Three RCs obtained by different methods are compared as shown in Fig. 9. For Tower-1, RCs are almost identical to each other. This is because that there are no large differences in SFCs. On the contrary, it can be seen that the proposed method can give RC quite similar to the one by the multi-event model. If RC by the multi-event model is assumed as correct since it is the precise method requiring no separation of hazard and fragility parts, the proposed method can be concluded that it also gives the better result than the previous method. It, of course, is noted that the proposed method requires less computational effort than the multi-event model.

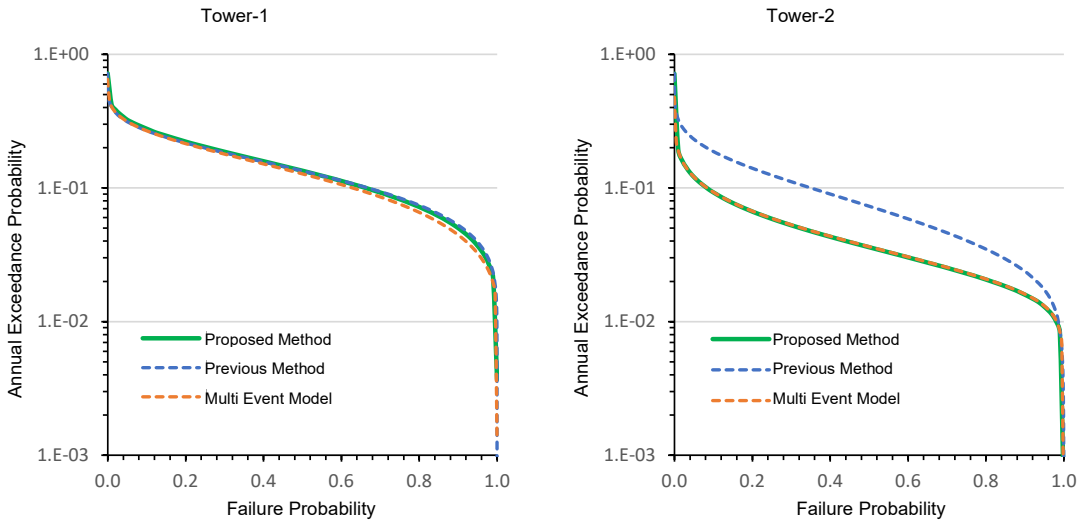

Figure 9. Adequacy of proposed method by comparing with results of multi-event model

In order to emphasize the effectiveness of proposed method, Fig. 10 shows the comparison of RCs by previous method and by proposed method. For the previous method, 4 type of SFCs are combined with SHC for all earthquakes as done in a usual risk analysis. For Tower-1, it is seen that all RCs are similar to each other. For Tower-2, it, however, must be noted that no RC is similar to the one by the proposed method that can be the true RC as stated above.

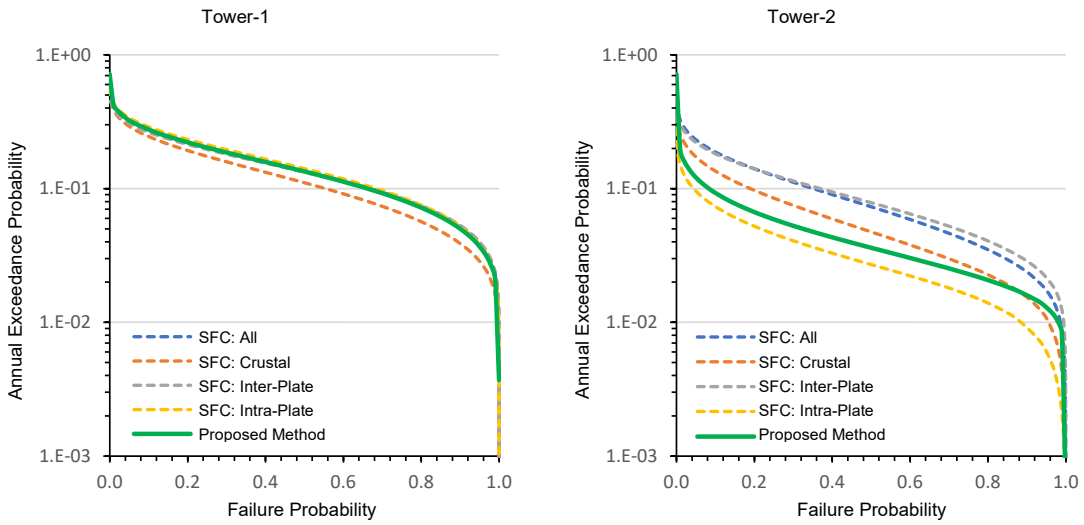

Figure 10. Effect of establishment of seismic fragility curve based on different earthquake type

CONCLUSION

Authors have conducted probabilistic risk evaluation of petrochemical plant structures using PGA as ground motion intensity. However, plant sites consist of various structures and equipment with various natural period, for which PGA is not a good risk estimator since it does not contain the information on spectral shape. So, this paper proposed the method by which the effect of spectral shape is introduced not in seismic hazard but in seismic fragility.

Two towers whose natural periods are 0.3s and 0.8s at Yokkaichi-site, Japan were selected as model structures for which earthquake-type dependent SFCs were established. At first, some sets of ground motions were developed based on the UHS at the site. Then seismic fragility curves of towers were developed by Monte-Carlo simulation using each set of ground motions.

The adequacy of establishing earthquake-type dependent SFCs is examined from the viewpoint of risk analysis, though this may be an indirect validation. Authors proposed the risk analysis method which combines the RCs of each earthquake type. This earthquake-type dependent RCs are obtained by earthquake-type dependent SFCs and SHCs. The RC by the proposed method has the good agreement of RC by the multi-event model, which is considered as the precise method.

In order to prove the adequacy of the proposed method, it will be applied to other sites where the crustal earthquakes or intra-plate earthquakes are dominant, as well as to the structures with different natural periods.

REFERENCES

Fukushima S. (2015). Risk analysis of portfolio of facilities using multi-event model, Transaction of 23rd SMiRT, Paper No.562

KHK (2012). Seismic Design Code of High-Pressure Gas Facilities, The High-Pressure Gas Safety Institute of Japan

NIED (2009). A Study on National Seismic Hazard Maps for Japan, *Technical Note of NIED No.336*, Japan. (in Japanese)

NIED (2019). Japan Seismic Hazard Information Station, http://www.j-shis.bosai.go.jp/en/, Japan.

Satoda, A., Oshima, M. (2017). Method for the evaluation of seismic risk and cost-effective strengthening of plant facilities, *Transaction of 24th SMiRT*, Busan, South Korea.

Tanaka, K., Wang, M., Takada, T. (2008). Covariance structure between spectral accelerations with different periods and its application, *J. Struct. Const. Eng.*, AIJ, Vol.73, No.632, 1727-1733. (in Japanese)